

($S \cdot V$), the optimum is (again) where $\partial \ln S / \partial \ln V = -1$ on the $\ln S$, $\ln V$ trade-off surface. This result is derived, but not really understood, in ref. 6.

It seems that several classic problems in life-history evolution yield a universal trade-off slope of -1 at the optimum because aggregated fitness (Box 1) is naturally expressed as a product of two allocation alternatives (E versus B , \bar{b} versus S , S versus V). Life histories are often treated as complex objects, with numerous possible age-dependent trade-offs^{7,8,15}. The approach here reduces them to just a few aggregate variables (S , \bar{b} , E)⁶. Although we sacrifice all information about age-dependent allocation decisions^{7,8}, we gain in finding general rules (hypotheses) about the shape of aggregate (average) trade-off surfaces at the equilibrium. I do not know of any data on trade-offs precise enough to test these differential-invariant predictions, particularly for the size/number or reproductive effort problems⁷. Theory for the optimal age at first reproduction using R_0 as a fitness measure often implicitly invokes the minus-one rule as an intermediate step in the prediction of attributes such as optimal adult body mass^{6,7,12}. Thus the minus-one rule is tested, at least qualitatively, whenever

these predictions work out. See, for example, the successful prediction of the heights and slopes of the between-species lifespan allometries for various mammal groups (ref. 6, p. 96; ref. 16). Of course, there are many qualitative (and a few quantitative) tests of product maximization for evolution of sex allocation^{2,6}.

The procedure described here is to reduce darwinian fitness to a function of a few aggregate variables, hoping to find a general form for fitness (here a product) which then yields general rules for the equilibrium. The trick is worth trying for other problems in phenotypic evolution. Economists often use this procedure and, indeed, production or utility function in the form of products are common; $X_1 \cdot X_2$, or more generally $X_1^A \cdot X_2^D$ (see any advanced text on price theory; A and D are > 0 and scale the relative productive value of inputs to X_1 and X_2 , respectively). Then products like that of equation (1) may often characterize fitness in non-growing populations with reproductive structure even more complex than simply age. □

Received 30 January; accepted 3 April 1997.

1. Parker, G. A. & Maynard Smith, J. Optimality theory in evolutionary biology. *Nature* **348**, 27–33 (1990).
2. Charnov, E. L. *The Theory of Sex Allocation* (Princeton Univ. Press, NJ, 1982).
3. Seger, J. & Stubblefield, J. W. in *Adaptation* 93–123 (Academic, New York, 1996).
4. Bulmer, M. G. *Theoretical Evolutionary Ecology* (Sinauer, Sunderland, MA, 1994).
5. Godfray, H. C. J. *Parasitoids* (Princeton Univ. Press, NJ, 1994).
6. Charnov, E. L. *Life History Invariants* (Oxford Univ. Press, 1993).
7. Stearns, S. C. *The Evolution of Life Histories* (Oxford Univ. Press, 1992).
8. Charlesworth, B. *Evolution in Age-Structured Populations*. (Cambridge Univ. Press, 1994).
9. Charnov, E. L. & Downhower, J. F. A trade-off-invariant life-history rule for optimal offspring size. *Nature* **376**, 418–419 (1995).
10. MacArthur, R. H. in *Theoretical and Mathematical Biology* (eds Waterman, T. H. & Morowitz, H.) 388–397 (Blaisdell, New York, 1965).
11. Williams, G. C. Natural selection, the cost of reproduction, and a refinement of Lack's principle. *Am. Nat.* **100**, 687–690 (1966).
12. Charnov, E. L. Evolution of life history variation among female mammals. *Proc. Natl Acad. Sci. USA* **88**, 1134–1137 (1991).
13. Lloyd, D. G. Selection of offspring size at independence and other size-versus-number strategies. *Am. Nat.* **129**, 800–817 (1987).
14. Mock, D. W. & Parker, G. A. *The Evolution of Sibling Rivalry* (Oxford Univ. Press, 1997).
15. Stearns, S. C. Tradeoffs in life history evolution. *Funct. Ecol.* **3**, 259–268 (1989).
16. Charnov, E. L. & Berrigan, D. Why do female primates have such long lifespans and so few babies? *Evol. Anthropol.* **1**, 191–194 (1993).

Acknowledgements. K. Hawkes, G. Parker, G. Getty and S. Proulx read and improved the arguments.

Correspondence and requests for materials should be addressed to the author.

Molecular basis of symbiosis between *Rhizobium* and legumes

Christoph Freiberg, Rémy Fellay*, Amos Bairoch†, William J. Broughton*, André Rosenthal & Xavier Perret*

Institut für Molekulare Biotechnologie, Abteilung Genomanalyse, Beutenbergstrasse 11, 07745 Jena, Germany

*Laboratoire de Biologie Moléculaire des Plantes Supérieures, Université de Genève, 1 ch. de l'Impératrice, 1292 Chambésy/Genève, Switzerland

† Biochimie Médicale, Centre Médical Universitaire, Université de Genève, 1 rue Michel-Servet, 1211 Genève 4, Switzerland

Access to mineral nitrogen often limits plant growth, and so symbiotic relationships have evolved between plants and a variety of nitrogen-fixing organisms. These associations are responsible for reducing 120 million tonnes of atmospheric nitrogen to ammonia each year. In agriculture, independence from nitrogenous fertilizers expands crop production and minimizes pollution of water tables, lakes and rivers. Here we present the complete nucleotide sequence and gene complement of the plasmid from *Rhizobium* sp. NGR234 that endows the bacterium with the ability to associate symbiotically with leguminous plants. In conjunction

Box 1 Fitness is a product

The 'net reproductive rate' R_0 , is defined as $R_0 = \int_0^{\infty} l(x) \cdot b(x) dx$, and calculates the average number of daughters produced over a female's lifespan. $l(x)$ is the probability of being alive at age x ; $b(x)$ is the daughters produced at age x who are alive at independence from mother; $b > 0$ only if $x > \alpha$, the age at first birth, measured from independence). Now, write $b(x) = b(y)$ for $y = x - \alpha$ and denote $l(x)$ for $x > \alpha$ as $l(x) = S(\alpha) \cdot e^{-\phi(x-\alpha)} = S(\alpha) \cdot e^{-\phi(y)}$. (Notice that $\phi(y)$ is zero at $y = 0$ and is increasing with y ; $a(-\log l(x))/dy = \partial \phi(y)/\partial y$, so $\partial \phi/\partial y$ is the instantaneous mortality rate at age y .) $S(\alpha)$ is the chance of living from independence to α . R_0 can be written for this general life history as

$$R_0 = S(\alpha) \cdot \int_0^{\infty} b(y) \cdot e^{-\phi(y)} dy \quad (2)$$

Recall from the stable age distribution theory that the proportion of the breeding lifespan spent between ages y and $y + dy$ (the probability density function for the adult ages) is given by

$$\frac{e^{-\phi(y)} dy}{\int_0^{\infty} e^{-\phi(y)} dy}$$

Now, multiply equation (2) by (1), written as

$$\frac{\int_0^{\infty} e^{-\phi(y)} dy}{\int_0^{\infty} e^{-\phi(y)} dy}$$

to yield

$$R_0 = S(\alpha) \left[\int_0^{\infty} b(y) \cdot \frac{e^{-\phi(y)}}{\int_0^{\infty} e^{-\phi(y)} dy} dy \right] \left(\int_0^{\infty} e^{-\phi(y)} dy \right) \quad (3)$$

$S(\alpha)$ is the chance of living to reproduce at age α ; while the term in square brackets is simply \bar{b} , the average rate of production of offspring over the reproductive adult life, and the term in curved brackets is simply $E(\alpha)$, the expectation of further life at age α , the average length of the adult lifespan. So equation (3) is really

$$R_0 = S(\alpha) \cdot \bar{b} \cdot E(\alpha) \quad (4)$$

Equation (4) applies to any age structured life history; R_0 is the simple product of three aggregated terms, each an average. For equation (4) to be used as a fitness measure, the population must not be growing. This makes $R_0 \approx 1$ for typical individuals owing to density dependence⁹. But mutant individuals may have their own $R_0 \neq 1$, and it is fitness and trade-offs for mutants which are discussed here. Thus we use R_0 , equation (4), as a fitness measure, with the condition that it must equal unity at the optimum, when mutants are the same as typical¹.

with transcriptional analyses, these data demonstrate the presence of new symbiotic loci and signalling mechanisms. The sequence and organization of genes involved in replication and conjugal transfer are similar to those of *Agrobacterium*, suggesting a recent lateral transfer of genetic information.

Many dissimilar organisms live in close association with one another. Nitrogen-fixing symbioses, in which auxotrophs exchange carbohydrates for organic nitrogen with diazotrophs, dominate numerous ecological niches. Members of the plant family Leguminosae, in association with the soil bacteria *Azorhizobium*, *Bradyrhizobium* and *Rhizobium*, are responsible for most of the nitrogen fixed biologically. Plant roots excrete a variety of substances, some of which (especially flavonoids) coordinate the expression of rhizobial nodulation (*nod*) genes¹. In turn, the Nod proteins direct synthesis of lipochito-oligosaccharidic Nod factors, which initiate nodule formation and allow rhizobia to enter the plant^{2,3}. Continued exchange of symbiotic signals is necessary for nitrogen fixation⁴.

As a general rule, symbiotic genes are plasmid borne in *Rhizobium* species and are located on the chromosome in *Azo* (*Brady*)*rhizobium* strains. To study the molecular control of broad host range in associations between legumes and *Rhizobium*, we use the fast-growing *Rhizobium* sp. NGR234 (ref. 5). This bacterium nodulates more than 110 genera of legumes, as well as the non-legume *Parasponia andersonii* (S. G. Pueppke and W.J.B., unpublished data), and possesses a large plasmid (pNGR234a) that carries most symbiotic determinants⁶. Using dye terminators and a thermostable sequenase⁷, we sequenced 20 cosmids from the canonical ordered library⁸, selected to cover pNGR234a.

The symbiotic replicon is 536,165 base pairs long (92% of the genome of *Mycoplasma genitalium*⁹). A total of 416 open reading frames (ORFs) were predicted to encode proteins (Fig. 1, Table 1), 139 of which show no similarity to any known protein. An additional 67 gene fragments were detected that seem to be remnants of functional genes. Many of these have clearly been disrupted by mobile elements. Collectively, potential genes and gene fragments make up 418 kilobases (78% of the replicon). This gene density is slightly lower than that of other bacterial genomes such as *Bacillus subtilis*, *Escherichia coli* and *Haemophilus influenzae*¹⁰ (85–92%; I. Moszer, personal communication), mostly because of the numerous insertion sequences and of their recombinatorial nature. No genes essential to transcription, translation or primary metabolism were found, which is consistent with the observation that NGR234 can be cured of its plasmid, giving strain ANU265 (ref. 11).

In total, 85 proteins belong to families that are represented more than once, even after discounting the many insertion-sequence encoded proteins or those involved in transposition, integration and recombination. There are some large families, including the five members of the short-chain dehydrogenase/reductases¹², one of which (y4vI) contains two homologous domains; four complete and one partial ABC-type transporter operons that each encode at least one ABC-type permease and ABC-type ATP-binding proteins; four cytochrome P450s; and three members of the peptidase family S9A.

Highest similarities were found with proteins of other rhizobia and agrobacteria. Only two eukaryotic proteins are highly homologous to pNGR234a counterparts. A glutamate dehydrogenase (y4uF) is significantly more closely related to the mitochondrial form than to that of prokaryotes or to archaea. As mitochondrial proteins are thought to originate from ancestral bacteria, y4uF could thus represent a new subclass of prokaryotic glutamate dehydrogenases. A small protein (y4sK), which belongs to a family (Prosite:PDOC00838) of uncharacterized proteins found in a variety of prokaryotes and eukaryotes, is more closely related to the known mammalian members of this family than to that of other prokaryotes.

Replication of pNGR234a probably begins at *oriV*, which is

located within the intergenic sequence between the *repC* (y4cI)- and *repB* (y4cJ)-like genes. This locus is highly similar (69–71%) to the origins of replication of *Agrobacterium* and *Rhizobium* plasmids (Fig. 2). In *Agrobacterium*, these intergenic sequences are the determinants of incompatibility. RepABC of pNGR234a are 40–60% identical to those of pTiB6S3 (a Ti-plasmid), pRiA4b (an Ri-plasmid) and pRL8JI (a cryptic *Rhizobium* plasmid). A 12-bp portion of the origin of transfer (*oriT*) is identical to that of pTiC58 of *A. tumefaciens*, and highly similar to those of RSF1010 (*E. coli*) and pTF1 (*Thiobacillus ferrooxidans*). This sequence corresponds to the *oriT* of plasmids containing the 'Q-type nick-region' (Fig. 3). Adjacent to this cluster are another 21 predicted genes that are homologous to the conjugal transfer genes of *Agrobacterium* Ti-plasmids. By marking the *nodD2* gene (y4xH), we were able to demonstrate high-frequency conjugal transfer of pNGR234a into ANU265. Conjugal transfer of Ti plasmids in *Agrobacterium* is controlled by a family of *N*-acyl-L-homoserine lactone auto-inducers^{13,14}. By using established methods¹⁴, we found similar molecules, which interact with the *Agrobacterium traR* gene product, in supernatants of NGR234 cultures.

Carbohydrates are not only constituents of the rhizobial cell wall: they are also morphogens. Short, *N*-acylated tri- to pentamers of *N*-acetyl-D-glucosamine (Nod factors) trigger nodulation responses in homologous legumes at very low concentrations¹⁵. Thus elements of the biosynthetic pathways leading to cell walls or to Nod factors are common. Most differences are found in the later stages of the pathways that yield specific cell-wall components or Nod factors. Yet even here, the distinction between structural and symbiotic carbohydrates is blurred. Specific extracellular polysaccharides (EPS) are required for nitrogen fixation in certain legume–*Rhizobium* associations¹⁶.

As befits a symbiotic replicon, only 10 ORFs with similarities to polysaccharide synthesis genes (*sensu stricto*) are plasmid borne (Table 1). Sequences homologous to *exo* genes are clearly located on the chromosome (X.P. and V. Viprey, unpublished data). Although loci with weak homologies to *nod*-box::*psiB* of *R. leguminosarum*, and *exoX* of *R. meliloti* exist on pNGR234a (y4iR, and y4xQ respectively), these are regulatory rather than structural.

Except for *nodE*, *nodG* and *nodPQ*, which are on the chromosome, most Nod-factor biosynthetic genes are plasmid borne, and are regulated by four transcriptional regulators of the *lysR* family: *nodD1* (y4aL), *syrm1* (y4pN), *nodD2* (y4xH) and *syrm2* (y4zF). Most *nod* genes share a conserved promoter sequence called the *nod* box. NodC (an *N*-acetylglucosaminyltransferase), which is the first committed enzyme in the Nod-factor biosynthetic pathway, is part of the *hsnIII* locus: *nodABCInolO* and *noeE* are responsible for synthesis of the core Nod factor as well as the adjunction of 3-(or 4)-*O*-carbomoyl-, 2-*O*-methyl-, and 4-*O*-sulphate¹⁷ groups, respectively (Fig. 4). The *hsnI* locus encodes enzymes involved in fucosylation of NodNGR factor¹⁸. NodS and NodU (*hsnII*) *N*-methylate and 6-*O*-carbomoylate NodNGR factors respectively¹⁹, whereas *noII* is probably an acetyltransferase.

We found 12 additional *nod* box-like sequences. Among these, two are upstream of the transcriptional regulators, *syrm2* and y4xI, and three (y4hM, *fixF* and y4iR) control expression of genes involved in polysaccharide metabolism. Transcription analysis suggests that at least 11 of the 17 putative *nod* boxes are symbiotically active (Fig. 1). Many *nod* box-dependent genes are under the direct control of NodD1, but y4wM is modulated by NodD2 (data not shown). The presence of both a *nod* box and a NifA- σ^{54} -type promoter upstream of y4vC suggests a new system of transcriptional regulation involving both flavonoid induction and expression in nodules (Fig. 5).

In contrast to the mosaic structure of the *nod* loci, pNGR234a contains a single large cluster of 43 *nif* and *fix* genes, including *nifA* (y4uN), which encodes a σ^{54} -dependent regulator. NifA contains two highly conserved regions, a carboxy-terminal part involved in

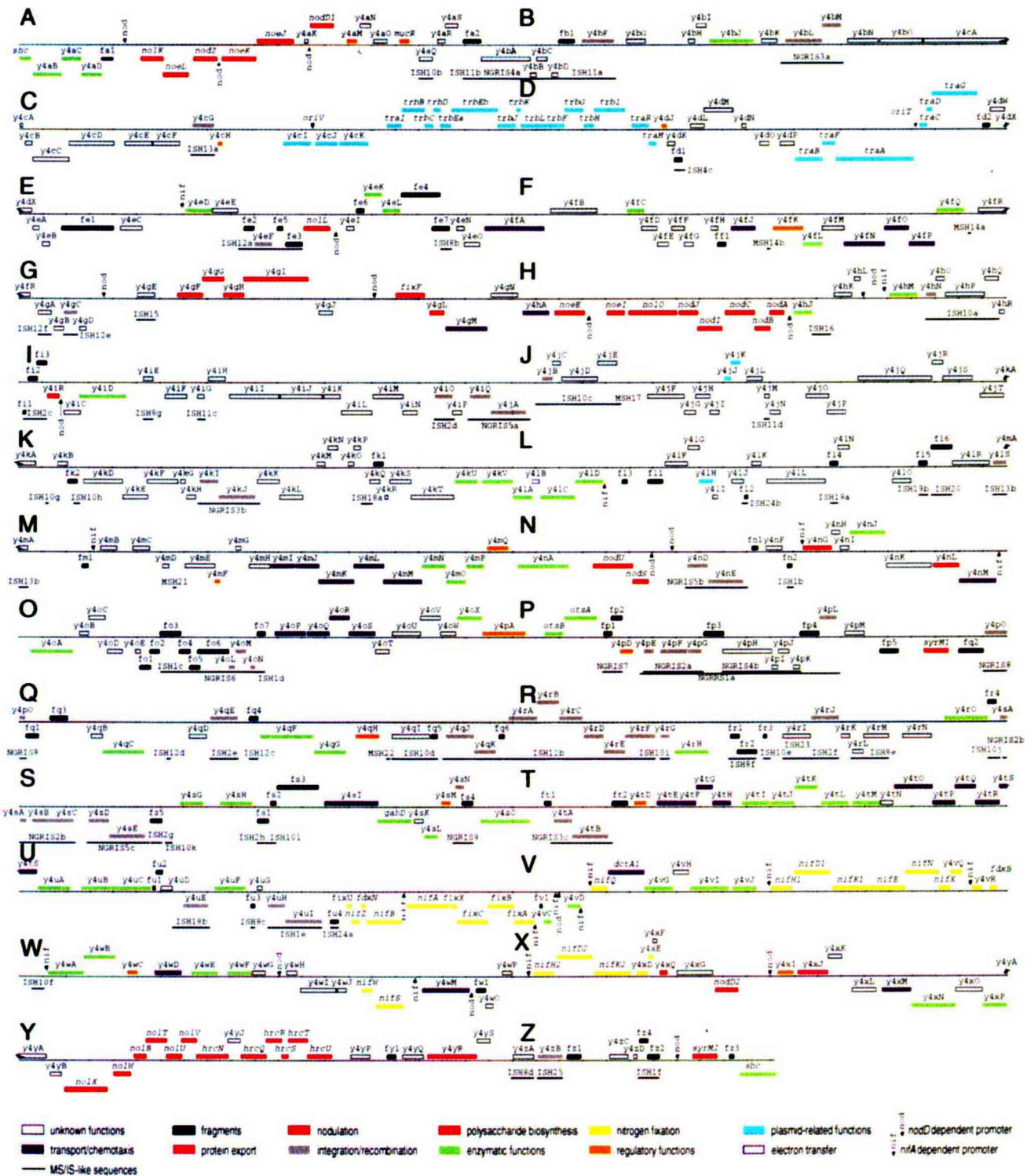


Figure 1 Genetic map of the symbiotic replicon pNGR234a. Each line represents 42 kb. ORF names (for example, y4aB) or the names of genes (for example, *shc*) correspond to those in Table 1. The third letter in each ORF name corresponds to one of 26 segments (A to Z), each of which is 21 kb in length except segment Z, which comprises 11,125 bp. The fourth letter of the ORF name indicates the position of the ORF within each segment (for example, y4gI is located on segment G between y4gH and y4gJ). Genes positioned on top of each line are transcribed from left to right, whereas those placed below the lines are encoded by the complementary strand. Colour-coded boxes represent putative coding regions

(and gene fragments) grouped according to their presumed functions, except for those involved in nodulation, polysaccharide synthesis, nitrogen fixation, and plasmid-related functions, which are grouped according to their phenotypic class (see Table 1). Positions of the origins of replication and transfer are marked *oriV* and *oriT*, respectively. Regions homologous to consensus sequences of *nod*-box- and *NifA*- σ^{54} dependent promoters are marked with a black arrowhead followed by *nod* and *nif*, respectively. Positions of insertion- and mosaic-sequences are annotated with lines (for example, ISH10b, NGR154a or MSH22).

DNA binding, and a central domain that interacts with an alternative sigma factor (σ^{54}) of the RNA polymerase. Mutation of *rpoN* (which encodes σ^{54}) causes a Fix⁻ phenotype on NGR234 hosts²⁰. Genes involved in the synthesis of the MoFe-nitrogenase complex are also present, including two identical copies of the *nifKDH* genes (*nifHDK1* and *nifHDK2*)²¹. Other *nif* and *fix* genes are involved in elaboration of the electron-transport complex (*fixA*, *fixB*), of various cofactors required for nitrogen fixation (*fixC*, *nifB*, *nifE*, *nifN*) and in the syntheses of ferredoxins (*fdxB*, *fdxN* and *fixX*). Although not directly involved in the fixation process, mutation of

the plasmid-borne copy of *dctA* (*dctA1*, *y4vF*) also impairs nitrogen fixation²².

In addition, 17 new genes expressed in nodules are part of this *nif* and *fix* cluster (*y4vC* to *y4vJ*, with the exception of *dctA1*, *y4wA* to *y4wG*, *y4wI*, *y4wJ* and *y4xQ*; see Fig. 5). The predicted functions of six of these (*y4vD*, *nifQ*, *y4vG*, *y4vI*, *y4vJ* and *y4wF*) suggest a role in electron transport and oxidation-reduction, but another five are not homologous to any database entry. It thus seems likely that most of the proteins necessary for bacteroid development and synthesis of the nitrogen-fixing complex are coded by pNGR234a, although



Figure 2 Multiple alignments of the nucleotide sequence of the replication origins of: the Ri plasmid of *Agrobacterium rhizogenes* (pRI44b); the symbiotic replicon of NGR234 (pNGR234a); the Ti plasmid of *A. tumefaciens* BS63 (pTiBS63); and pRL8JI of *R. leguminosarum* bv. *leguminosarum* (pRL8JI). Gaps introduced to give the best sequence alignments are marked with hyphens.

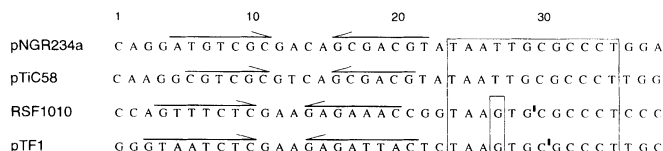


Figure 3 Multiple DNA sequence alignments of loci containing the origin of transfer of: the symbiotic plasmid of NGR234 (pNGR234a); the Ti plasmid of *A. tumefaciens* C58 (pTiC58); a mobilizable plasmid of *E. coli* (RSF1010) and a mobilizable plasmid of *Thiobacillus ferrooxidans* (pTFI). Major conserved nucleotide residues are boxed. Known 'nick' sites corresponding to the nucleotide positions where the specific plasmid strand is cleaved are marked with black boxes. Sequence features in the trailing portion of the *oriT* sites include inverted repeats, which are marked with horizontal arrows.

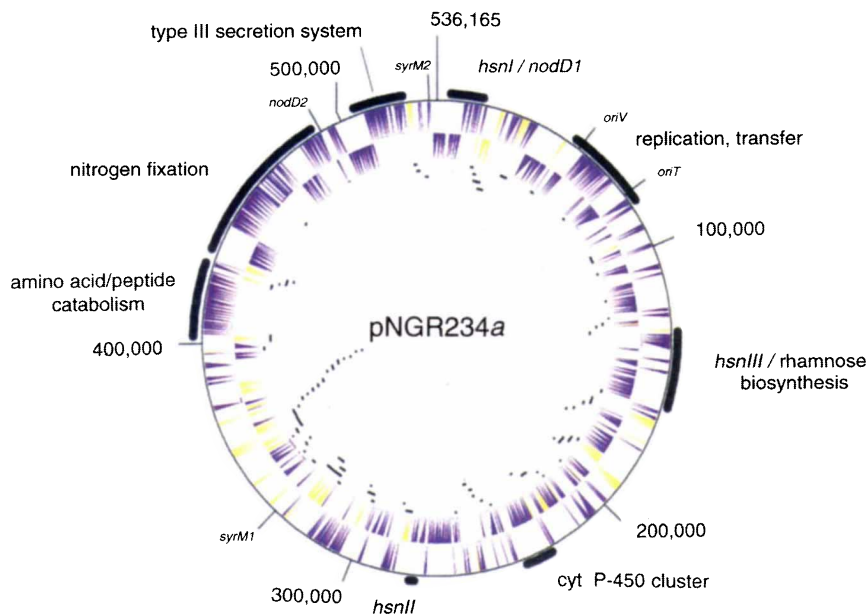


Figure 4 Circular representation of pNGR234a. Outer and inner concentric circles indicate coding regions identified on the plus and minus strands, respectively. Within these predicted genes, those coloured in yellow correspond to ORFs that belong to insertion-like elements. Thin concentric black lines represent mosaic

sequences as well as complete or partial insertion sequence-like repeats. Major gene clusters are highlighted as thick black concentric lines (for example, *hsn*, host specificity of nodulation loci).

Table 1 Functional and phenotypic classification of the predicted proteins encoded by pNGR234a

| general statistics | | proteins sorted according to phenotypic classes | | other proteins | |
|--|--------|---|--------------------|------------------------------------|--------------------|
| | | functional class | number of proteins | functional class | number of proteins |
| total number of predicted proteins | 416 | nodulation | | various enzymatic functions | 59 |
| mean length of the putative proteins (smallest: 43 aa, largest: 1197 aa) | 308 aa | enzymes | 14 | transport | 29 |
| putative subcellular locations of the predicted proteins: | | transporters | 2 | protein export/secretion | 8 |
| - cytoplasmic | 329 | transcriptional regulators | 4 | chemotaxis | 2 |
| - transmembrane (inner membrane) | 62 | export proteins | 1 | electron transfer | 1 |
| - periplasmic | 20 | unknown functions | 5 | transcriptional regulation | 14 |
| - outer membrane | 2 | poly- / oligosaccharide synthesis | | integration/recombination | 44 |
| - lipoprotein attached to a membrane | 3 | enzymes | 9 | | |
| number of proteins grouped into functional classes | 234 | transcriptional regulators | 1 | | |
| number of unknown proteins: | | nitrogen fixation | | | |
| - with database homolog | 43 | enzymes | 13 | | |
| - without any database homolog | 139 | electron transfer proteins | 5 | | |
| | | transcriptional regulators | 1 | | |
| | | unknown functions | 7 | | |
| | | plasmid-related functions / cell development | | | |
| | | enzymes | 1 | | |
| | | export proteins | 12 | | |
| | | transcriptional regulators | 2 | | |
| | | plasmid control/cell development proteins | 12 | | |

| ORF name | gene name | description of the predicted protein | |
|--|-------------|--|---|
| nodulation | | | |
| Nod-factor biosynthesis/modification/transport | | | |
| y4A | <i>noIK</i> | pu. NAD-dependent nucleotide sugar epimerase/dehydrogenase | y4uP <i>fixC</i> nitrogenase cofactor biosynthesis |
| y4A | <i>noeL</i> | GDP-mannose 4,6-dehydratase | y4vA <i>fixB</i> electron transfer fixAB complex |
| y4A | <i>nodZ</i> | fucosyltransferase | y4vB <i>fixA</i> electron transfer fixAB complex |
| y4A | <i>noeK</i> | phosphomannomutase | y4vE <i>nifQ</i> pu. nitrogenase Mo cofactor processing |
| y4A | <i>noeJ</i> | mannose-1-phosphate guanylyltransferase | y4vK <i>nifH1</i> nitrogenase Fe protein; id. to y4XA |
| y4E | <i>noIL</i> | sim. to <i>R. loti</i> acetyltransferase NoIL | y4vL <i>nifD1</i> nitrogenase MoFe protein alpha subunit; id. to y4XB |
| y4H | <i>noeE</i> | transfer of activated sulfate to fucose | y4vM <i>nifK1</i> nitrogenase MoFe protein beta subunit; id. to y4XC |
| y4C | <i>noel</i> | not yet characterized step in Nod-factor synthesis | y4vN <i>nifE</i> nitrogenase MoFe cofactor synthesis |
| y4D | <i>noO</i> | O-carbamoylation of Nod-factors | y4vO <i>nifN</i> nitrogenase MoFe cofactor synthesis |
| y4E | <i>nodJ</i> | pr. ABC transporter permease | y4vP <i>nifX</i> unknown function |
| y4F | <i>nodI</i> | pr. ABC transporter ATP-binding protein | y4vQ <i>nifW</i> sim. to <i>nifX-nifW</i> intergenic ORF in nitrogen-fixing bacteria |
| y4G | <i>nodC</i> | N-acetylglucosaminyltransferase | y4vR <i>fdxB</i> 4Fe-4S ferredoxin |
| y4H | <i>nodB</i> | chitoooligosaccharide deacetylase | y4vS <i>nifW</i> unknown function |
| y4I | <i>nodA</i> | N-acetyltransferase | y4vK <i>nifS</i> class-5 aminotransferase |
| y4N | <i>nodU</i> | 6-O-carbamoylation of Nod-factors | y4vL <i>nifS</i> nitrogenase Fe protein; id. to y4vK |
| y4C | <i>nodS</i> | methyltransferase involved in Nod-factor synthesis | y4xB <i>nifD2</i> nitrogenase MoFe protein alpha subunit; id. to y4vL |
| | | | y4xC <i>nifK2</i> nitrogenase MoFe protein beta subunit; id. to y4vM |
| | | | y4xD <i>nifW</i> sim. to <i>nifX-nifW</i> intergenic ORF in nitrogen-fixing bacteria |
| | | | y4xE <i>nifW</i> sim. to <i>nifX-nifW</i> intergenic ORF in nitrogen-fixing bacteria |
| | | | plasmid-related functions / cell development |
| | | | y4cI pu. replication protein; sim. to <i>A. rhizogenes</i> repC |
| | | | y4cJ pu. replication protein; sim. to <i>A. rhizogenes</i> repB |
| | | | y4cK pu. replication protein; sim. to <i>A. rhizogenes</i> repA |
| | | | y4cL <i>traI</i> pr. autoinducer synthetase |
| | | | y4cM <i>trbB</i> pr. conjugal transfer protein (PuIE family) |
| | | | y4cN <i>trbC</i> pr. conjugal transfer protein (export prot.) |
| | | | y4cO <i>trbD</i> pr. conjugal transfer protein (export prot.) |
| | | | y4cP <i>trbEa</i> pr. conjugal transfer protein (export prot.) |
| | | | y4cQ <i>trbEb</i> pr. conjugal transfer protein (export prot.) |
| | | | y4dA <i>trbJ</i> pr. conjugal transfer protein (export prot.) |
| | | | y4dB <i>trbK</i> pr. conjugal transfer protein (export prot.) |
| | | | y4dC <i>trbL</i> pr. conjugal transfer protein (export prot.) |
| | | | y4dD <i>trbF</i> pr. conjugal transfer protein (export prot.) |
| | | | y4dE <i>trbG</i> pr. conjugal transfer protein (export prot.) |
| | | | y4dF <i>trbH</i> pr. conjugal transfer protein (export prot.) |
| | | | y4dG <i>trbI</i> pr. conjugal transfer protein (export prot.) |
| | | | y4dH <i>traR</i> LuxR family H-T-H regulator |
| | | | y4dI <i>traM</i> pu. repressor |
| | | | y4dQ <i>traB</i> pr. conjugal transfer protein |
| | | | y4dR <i>traF</i> pr. conjugal transfer protein |
| | | | y4dS <i>traA</i> pr. conjugal transfer protein |
| | | | y4dT <i>traC</i> pr. conjugal transfer protein |
| | | | y4dU <i>traD</i> pr. conjugal transfer protein |
| | | | y4dV <i>traG</i> pr. conjugal transfer protein |
| | | | y4jI pu. plasmid stability protein; sim. to <i>Ps. syringae</i> StbC |
| | | | y4jK pu. plasmid stability protein; sim. to <i>Ps. syringae</i> StbB |
| | | | y4lH pu. cell filamentation protein; sim. to enterobacterial protein Fic |
| | | | various enzymatic functions |
| | | | y4aA <i>shc</i> pr. squalene-hopene cyclase |
| | | | y4aC pu. phytoene synthase |
| | | | y4aD sim. to phytoene synthases |
| | | | y4bJ pu. peptidase (S2C family) |
| | | | y4eD pu. phosphodiesterase |
| | | | y4eK pr. short chain oxidoreductase |
| | | | y4eL pr. short chain oxidoreductase |
| | | | y4fC* pu. monooxygenase |
| | | | y4fL member of inositol monophosphatase family |
| | | | y4fQ 'ROK' family member |
| | | | y4gN sim. to <i>V. anguillarum</i> VirA |
| | | | y4hJ* pu. oxidoreductase; sim. to N-terminus of anaerobic coproporphyrinogenIII oxidases |
| | | | y4hM pu. oxidoreductase; Low similarity to <i>Z. mobilis</i> glucose-fructose oxidoreductase |
| | | | y4iD pr. monooxygenase |
| | | | y4kU pr. geranyltransferase |
| | | | y4kV pr. cytochrome P450 |
| | | | y4lA pr. short chain oxidoreductase |
| | | | y4lC pr. cytochrome P450 |
| | | | y4lD pr. cytochrome P450 |
| | | | y4mN* pr. TPP enzyme (transketolase family; C-terminus) |
| | | | y4mO* pr. TPP enzyme (transketolase family; N-terminus) |
| | | | y4mP pr. short chain oxidoreductase |
| | | | y4nA pr. peptidase (S9A family) |
| | | | y4nJ pr. GMC-type oxidoreductase |
| | | | y4oA sim. to <i>E. coli</i> pMCCC7 microcin biosynthesis protein MccB |
| | | | y4cX pr. NAD-dependent oxidoreductase |
| | | | y4pB <i>otsB</i> pr. trehalose-phosphatase |
| | | | y4pC <i>otsA</i> pr. α,α -trehalose-phosphate synthase |
| | | | y4cQ sim. to <i>E. coli</i> pMCCC7 microcin biosynthesis protein MccB |
| | | | y4qF pr. peptidase (S9A family) |
| | | | y4qG class-3 aminotransferase |
| | | | y4rH pu. ligase; sim. to biotin carboxylase |
| | | | y4rO pu. C-terminus of histidinol-phosphate aminotransferase |
| | | | y4sG pu. ligase; sim. to D-ala, D-ala ligases |
| | | | y4sH pu. cell wall compound biosynthesis protein; sim. to <i>B. anthracis</i> CapA |
| | | | y4sJ <i>gabD</i> pr. succinate-semialdehyde dehydrogenase |
| | | | y4sL pu. oxidoreductase; sim. to C-terminus of <i>E. coli</i> D-amino acid dehydrogenase small subunit |
| | | | y4sO pr. peptidase (S9A family) |
| | | | y4tI pu. peptidase (M40 family) |
| | | | y4tJ pu. threonine dehydratase |
| | | | y4tK pu. cyclodeaminase |
| | | | y4tL pu. peptidase/hydrolase (M24 family) |
| | | | y4tM pu. peptidase/hydrolase (M24 family) |
| | | | y4uA pu. cell wall comp. biosynthesis protein; sim. to <i>B. anthracis</i> CapA |
| | | | y4uB class-3 aminotransferase |
| | | | y4uC pr. aldehyde dehydrogenase |
| | | | y4uF pr. glutamate dehydrogenase |
| | | | y4vC member of HesB/YadR/YfhF family |
| | | | y4vD pu. redox enzyme; sim. to <i>C. bovidii</i> peroxisomal proteins A/B & <i>H. influenzae</i> H10572 |
| | | | y4vG pr. cytochrome P450 |
| | | | y4vI pr. short chain oxidoreductase |
| | | | y4vJ pu. monooxygenase; sim. to LuxA/B (bacterial luciferase) |
| | | | y4wA pr. zinc peptidase (M16 family) |
| | | | y4wB pu. zinc peptidase (M16 family) |
| | | | y4wE class-2 aminotransferase |
| | | | y4wF pu. monooxygenase; sim. to LuxA/B (bacterial luciferase) |

Table 1 continued

| | | | | | |
|--|---|--|---|--|---|
| y4xN | Low similarity to <i>E. coli</i> pCOLV-K30 | y4iO* | pu. transposase (sim. to IS1111A/IS1328/IS1533 family) | y4iC | sim. to <i>M. tuberculosis</i> Mtcy373.06 |
| y4xP | aerobactin synthase subunit lucC pu. cysteine synthase | y4iQ | pu. transposase-associated ATP-binding protein; id. to y4nD & y4sD (sim. to IS21/IS1162 family) | y4iL | pr. AAA-family ATPase |
| transport | | y4jA | pu. transposase; id. to y4nE & y4sE (sim. to IS21/IS1162 family) | y4kR* | sim. to N-terminus of <i>Erw. herbicola</i> ORF6 in <i>crtE-crx</i> region |
| probable sugar transport systems | | y4jB | sim. to IS elements IS2/IS1312/IS866 proteins | y4kS | highly sim. to <i>Br. japonicum</i> hyp. protein |
| y4mI | pr. ABC transporter binding prot. | y4jK | pu. transposase; id. to y4bL & y4tB (sim. to IS21/IS1162 family) | y4kT | highly sim. to <i>Br. japonicum</i> hyp. protein |
| y4mJ | pr. ABC transporter permease | y4kI | pu. transposase-associated ATP-binding protein; id. to y4bM & y4tA (sim. to IS21/IS1162 family) | y4lL | Member of <i>E. coli</i> YegE/YhdA/YjhK/YjcC family |
| y4mK | pr. ABC transporter ATP-binding protein | y4kL | pu. integrase/recombinase 'resolvase-type' | y4lO | sim. to <i>Ps. syringae</i> avirulence protein AvrRxv |
| y4oP | pr. ABC transporter binding protein | y4kN | pu. transposase; id. to y4bL & y4tB (sim. to IS21/IS1162 family) | y4mB | sim. to <i>E. coli</i> yciD; <i>V. cholerae</i> OmpW & <i>Ps. oleovorans</i> AikL |
| y4oQ | pr. ABC transporter permease | y4kO | pu. integrase/recombinase 'phage-type' | y4mE | sim. to <i>E. coli</i> HipA & <i>H. influenzae</i> HI0665 |
| y4oR | pr. ABC transporter permease | y4kP | pr. transposase; id. to y4sB (sim. to IS1111A/IS1328/IS1533 family) | y4nH | sim. to <i>E. coli</i> ethidium bromide resistance protein MvrC |
| y4oS | pr. ABC transporter ATP-binding protein | y4kQ | sim. to <i>A. xylinum</i> IS1268 ORFA; id. to y4sC | y4rN | sim. to <i>M. tuberculosis</i> Mtcy50.24 |
| probable aminoacid/peptide transport systems | | y4kR | sim. to <i>R. fredii</i> RFRS9 and <i>Azo. xylinum</i> IS1268 ORF; id. to y4sA | y4sK | pr. important cellular function (Yer057C/Y1051C/YjgF family) |
| y4tE | pr. ABC transporter binding protein | y4kS | pr. transposase; id. to y4jA & y4sE (sim. IS21/IS1162 family) | y4wH | sim. to <i>A. tumefaciens</i> plasmid pTIA6 ORF in pinF2 region |
| y4tF | pr. ABC transporter permease | y4pE | sim. to <i>R. fredii</i> RFRS9 and <i>Azo. xylinum</i> IS1268 ORF; id. to y4sA | y4yJ | sim. to <i>R. fredii</i> USDA257 ORF7 |
| y4tG | pr. ABC transporter permease | y4pF | pr. transposase; id. to y4sB (sim. to IS1111A/IS1328/IS1533 family) | y4zC | sim. to <i>Ps. syringae</i> avirulence protein AvrPph3 |
| y4tH | pr. ABC transporter ATP-binding protein | y4pG | sim. to <i>A. xylinum</i> IS1268 ORFA; id. to y4sC | unknown function | |
| y4tO | pr. ABC transporter binding protein | y4pL | pu. transposase-associated ATP-binding protein (sim. to IS21/IS1162 family) | (no database homologue) | |
| y4tP | pr. ABC transporter permease | y4pO | pr. transposase (Mutator family) | derived from IS element-like sequences | |
| y4tQ | pr. ABC transporter permease | y4qE | pr. transposase (sim. to IS1111A/IS1328/IS1533 family) | y4bA | id. to y4pH |
| y4tR | pr. ABC transporter ATP-binding protein | y4qJ | pu. transposase (sim. to IS801) | y4bB | id. to y4pl |
| y4tS | pr. ABC transporter ATP-binding protein | y4qK | pu. integrase/recombinase 'phage-type' | y4bC | id. to y4pj |
| other transport systems | | y4rA | pu. integrase/recombinase 'phage-type' | y4bD | id. to y4pK |
| y4fJ | pu. porin; sim. to <i>R. leguminosarum</i> OMP111A | y4rB | pu. integrase/recombinase 'phage-type' | y4gA | |
| y4fN | pr. ABC transporter permease | y4rC | pu. integrase/recombinase 'phage-type' | y4gE* | |
| y4fO | pr. ABC transporter ATP-binding protein | y4rD | pu. integrase/recombinase 'phage-type' | y4iE* | |
| y4fP | pr. ABC transporter binding protein | y4rE | pu. integrase/recombinase 'phage-type' | y4iG* | |
| y4gM | pr. ABC transporter ATP-binding protein | y4rF | pu. integrase/recombinase 'phage-type' | y4iP* | |
| y4hA | pu. ionic transporter; sim. to <i>E. coli</i> ChaA | y4rG | pu. integrase/recombinase 'phage-type' | y4jM* | |
| y4mL | pu. permease (<i>E. coli</i> YiaN/YgiK family) | y4rI | sim. to IS2/IS1312/IS866 proteins | y4kQ* | |
| y4mM | pu. permease (SBR family 7) | y4sA | sim. to <i>R. fredii</i> RFRS9 and <i>Azo. xylinum</i> IS1268 ORF; id. to y4pE | y4mA | |
| y4nM | pu. permease; sim. to <i>Az. cauldans</i> NoeC | y4sB | pr. transposase; id. to y4pF (sim. to IS1111A/IS1328/IS1533 family) | y4mC | |
| y4vF | <i>dctA1</i> C4-dicarboxylate transporter | y4sC | sim. to <i>A. xylinum</i> IS1268 ORFA; id. to y4pG | y4nO | |
| y4wD | permease-type protein; sim. to <i>R. meliloti</i> MosC | y4sD | pu. transposase-associated ATP-binding protein; id. to y4iQ & y4nD (sim. to IS21/IS1162 family) | y4pH | id. to y4bA |
| y4wM | pu. ABC transporter binding prot. | y4sE | pu. transposase; id. to y4jA & y4nE (sim. to IS21/IS1162 family) | y4pl | id. to y4bB |
| y4xM | <i>permease-type protein</i> ; sim. to <i>E. coli</i> YceE and to tetracycline transporters | y4sN | pu. transposase (IS6501 family) | y4pj | id. to y4bC |
| protein export/secretion | | y4tA | pu. transposase-associated ATP-binding protein; id. to y4bM & y4kI (sim. to IS21/IS1162 family) | y4pK | id. to y4bD |
| y4yl | <i>hrcN</i> pr. ATP synthase of a secretion system | y4tB | pu. transposase; id. to y4bL & y4kI (sim. to IS21/IS1162 family) | y4rI | |
| y4yK | <i>hrcQ</i> pr. secretion system protein (FliiN/MopA/SpaO family) | y4uH | pu. transposase-associated ATP-binding protein (sim. to IS21/IS1162 family) | y4rL* | |
| y4yL | <i>hrcR</i> pr. secretion system protein (FliP/MopC/SpaP family) | y4uJ | pu. transposase (sim. to IS21/IS1162 family) | y4rM* | |
| y4yM | <i>hrcS</i> pr. secretion system protein (FliQ/MopD/SpaQ family) | y4uE* | pu. transposase (sim. to IS110 family) | y4zA* | |
| y4yN | <i>hrcT</i> pr. secretion system protein (FliR/MopE/SpaR family) | y4zB* | pu. transposase (sim. to IS4 family) | | |
| y4yO | <i>hrcU</i> pr. secretion system protein (FliH/HrpN/SpaS family) | unknown function | | | |
| y4yR | pr. secretion system protein (FHIPEP family) | (with database homologue) | | | |
| y4xJ | secretion system protein (PulD family) | derived from IS element-like sequences | | | |
| chemotaxis | | y4aQ | sim. to ORFs in <i>R. meliloti</i> & <i>A. tumefaciens</i> Ti plasmid | not linked to IS elements | |
| y4fA | pr. chemoreceptor | y4hO | sim. to ORF from <i>R. leguminosarum</i> symbiotic plasmid | y4aK | y4iH |
| y4sI | pr. chemoreceptor | y4hP | sim. to ORFs in <i>R. meliloti</i> & <i>A. tumefaciens</i> Ti plasmid | y4aL | y4iI |
| electron transfer | | y4hQ | sim. to ORF-3 in <i>A. rhizogenes</i> plasmid pRI4A4B | y4aO | y4mD |
| y4iB | pu. 3Fe-3S ferredoxin | y4jC | sim. to ORF from <i>R. leguminosarum</i> symbiotic plasmid | y4aP | y4mG |
| transcriptional regulation | | y4jD | sim. to ORFs in <i>R. meliloti</i> & <i>A. tumefaciens</i> Ti plasmid | y4aR | y4mH |
| y4aM | pu. DNA-binding protein according to <i>Rsp. rubrum</i> protein homologue | y4qI | sim. to ORFs in <i>R. meliloti</i> & <i>A. tumefaciens</i> Ti plasmid | y4aS | y4nF |
| y4aP | mucR Ros/MucR homologue | not linked to IS elements | | y4aT | y4nG |
| y4cH | pr. cold shock regulator | y4aN | sim. to <i>A. rhizogenes</i> pRI4A4B replication region ORF3 | y4aU | y4nH |
| y4dJ | PbsX family H-T-H regulator | y4bI | sim. to <i>H. influenzae</i> HI1631 | y4aV | y4nI |
| y4fK | AraC family H-T-H regulator | y4bK | sim. to <i>Ps. aeruginosa</i> PAH cluster ORF1 | y4aW | y4nK |
| y4mF | pr. H-T-H regulator; sim. to phage p22 C2 | y4dO* | sim. to mitochondrial intron encoded ORFs & <i>E. coli</i> ORF319 | y4aX | y4nL |
| y4mQ | LysR family H-T-H regulator | y4dP | sim. to <i>A. tumefaciens</i> Ti plasmid ORF2&3 in conjugal transfer region 1 | y4aY | y4nM |
| y4pA | pr. sigma54-dependent H-T-H regulator | y4eC | sim. to N-terminus of <i>E. coli</i> pRP4 & pR751 Trac | y4aZ | y4nN |
| y4pD | Ros/MucR homologue | y4fR | sim. to <i>Sh. flexneri</i> lpaH 7.8 & <i>Y. pestis</i> YopM | | |
| y4qH | LuxR family H-T-H regulator | | | | |
| y4sM* | AsnC/Lrp family H-T-H regulator | | | | |
| y4tD | AsnC/Lrp family H-T-H regulator | | | | |
| y4wC | pu. DNA-binding protein according to <i>Rsp. rubrum</i> protein homologue | | | | |
| y4xI | Signal transduction-type regulator | | | | |
| integration/recombination | | | | | |
| y4bF | pu. transposase (sim. to IS1202) | | | | |
| y4bL | pu. transposase; id. to y4kI & y4tB (sim. to IS21/IS1162 family) | | | | |
| y4bM | pu. transposase-associated ATP-binding protein; id. to y4kI & y4tA (sim. to IS21/IS1162 family) | | | | |
| y4cG | pr. DNA invertase 'resolvase-type' | | | | |
| y4eF | pu. integrase/recombinase 'phage-type' | | | | |
| y4gC | pu. integrase/recombinase 'phage-type' | | | | |
| y4hN | sim. to IS2/IS1312/IS866 proteins | | | | |

The nomenclature system for the ORFs is described in the Fig. 1 legend. General abbreviations: amino acids (aa), identical (id.), probable (pr.), putative (pu.), similar (sim.), hypothetical (hyp.), thiamine pyrophosphate (TPP), alanine (ala), insertion sequence (IS). Abbreviations of organisms: *Agrobacterium* (A.), *Azotobacter* (Az.), *Bacillus* (B.), *Bradyrhizobium* (Br.), *Candida* (C.), *Desulfovibrio* (D.), *Escherichia* (E.), *Erwinia* (Erw.), *Haemophilus* (H.), *Mycobacterium* (M.), *Mycrococcus* (Myx.), *Pseudomonas* (Ps.), *Rhizobium* (R.), *Rhodospirillum* (Rsp.), *Shigella* (Sh.), *Streptomyces* (St.), *Vibrio* (V.), *Zymomonas* (Z.). Asterisk indicates possibly fragmentous gene.

some essential *fix* loci are probably carried on the chromosome²³ (V. Viprey, personal communication).

One way of gaining insight into the function of genes is to follow their expression under different conditions. To do this, RNA was hybridized against filters containing amplified portions of 113 genes and gene fragments stretching from y4uA to y4bA. Under the conditions tested, transcripts were produced from most of the ORFs, but only a few genes are expressed in liquid medium (Fig. 5). Induction with daidzein rapidly increased transcript levels of y4vC, y4xL, y4xO, y4yB, y4yP, fy1, y4yQ (all of unknown function), y4xP (cysteine synthase) and y4zF (*syrM2*). Others, such as y4wF (a putative monooxygenase), y4wE (an aminotransferase), y4wM (an ABC-transporter binding protein), y4xI (a signal transduction-type regulator), y4xK (unknown), as well as *nolBTUV* and *hrcNQRST* are induced later. As expected, those genes involved in nitrogen fixation (both copies of *nifKDH*, and *nifE*), as well as y4wA, y4wb (which encodes zinc peptidases), y4wC (a DNA-binding protein), y4wD (a permease), y4aP (*mucR*) and y4aQ (unknown) are strongly expressed in nodules.

In addition to bacterial Nod factors, other signal molecules are probably necessary for the establishment of an effective symbiosis. This is exemplified by a rhamnose-rich extracellular polysaccharide that is involved in bacteroid development and nitrogen fixation in *Vigna*. A single locus encodes the complete biosynthetic pathway of dTDP-rhamnose from glucose-1-phosphate (y4gH, y4gF, y4gI, y4gJ and *fixF*), while the y4gI gene product is probably needed for synthesis of rhamnose-rich lipopolysaccharides from dTDP-rhamnose²⁴.

Polypeptides and proteins are also probably involved in symbiosis. Six ORFs downstream of *nolXWBTUV* show strong homology to components of the type III secretion machinery of animal and plant pathogens. Homologues of these genes (*hrcN*, y4yJ, *hrcQ*, *hrcR*, *hrcS*, *hrcT* and *hrcU*) are responsible for secretion of various proteins, and have been sequenced in the closely related bacterium *R. fredii* strain USDA257 (EMBL accession no. L12251). Secretion of

five genistein-induced proteins of USDA257 is dependent on a functional *nolXWBTUV* locus²⁵. Both in mammalian and plant pathogens, most of the proteins exported by the type III secretion machinery are pathogenicity determinants. Homologues of YopM of *Yersinia pestis* (y4fR), as well as avirulence genes of *Pseudomonas syringae* (y4lO) and *Xanthomonas campestris* (y4zC), were also found, reinforcing the idea that symbiotic and pathogenic interactions share common molecular mechanisms.

Surprisingly, mosaic sequences and insertion sequences comprise 18% of pNGR234a, and resemble those of diverse eubacteria (*Agrobacterium*, *Bacillus*, *Escherichia*, *Pseudomonas* and *Rhizobium*). Many are clustered between nucleotides 300,000 and 390,000 (Fig. 1). Other insertion and mosaic sequences divide the replicon into large blocks of functionally related genes (*oriV-oriT*, *nif*, *fix*, *hsn*; Fig. 4), suggesting that NGR234 has functioned as a 'transposon trap'. The G+C contents of these insertion and mosaic sequences are 3% higher than that of pNGR234a (58.5%) which, in turn, is 3.7 mol% less than the 62.2 mol% calculated for the entire genome²⁶. Several genes, especially those involved in Nod-factor and polysaccharide synthesis, have low G+C contents (45–55 mol%), raising the possibility that *nod* genes evolved separately from *nif* and *fix* genes (G+C content, 59 mol%). Although transposition of these insertion elements has not been demonstrated, transfer of plasmids amongst rhizobia in the legume rhizosphere²⁷ and to other non-symbiotic bacteria in fields²⁸ indicates that lateral transfer of genetic information has helped model symbiotic potential.

The high proportion of insertion and mosaic sequences and the well-conserved *Agrobacterium* conjugal transfer loci have broad implications for the evolution of symbioses between legumes and *Rhizobium*. Both genera are closely related²⁹, and the similarity of basic plasmid functions suggests a common origin. It is thus possible that an *Agrobacterium*-like progenitor gathered symbiotic genes through transposition with other soil bacteria, or that the progenitor was *Rhizobium* which assimilated opine and hormone genes from the plant³⁰. Transposable elements shape evolution in

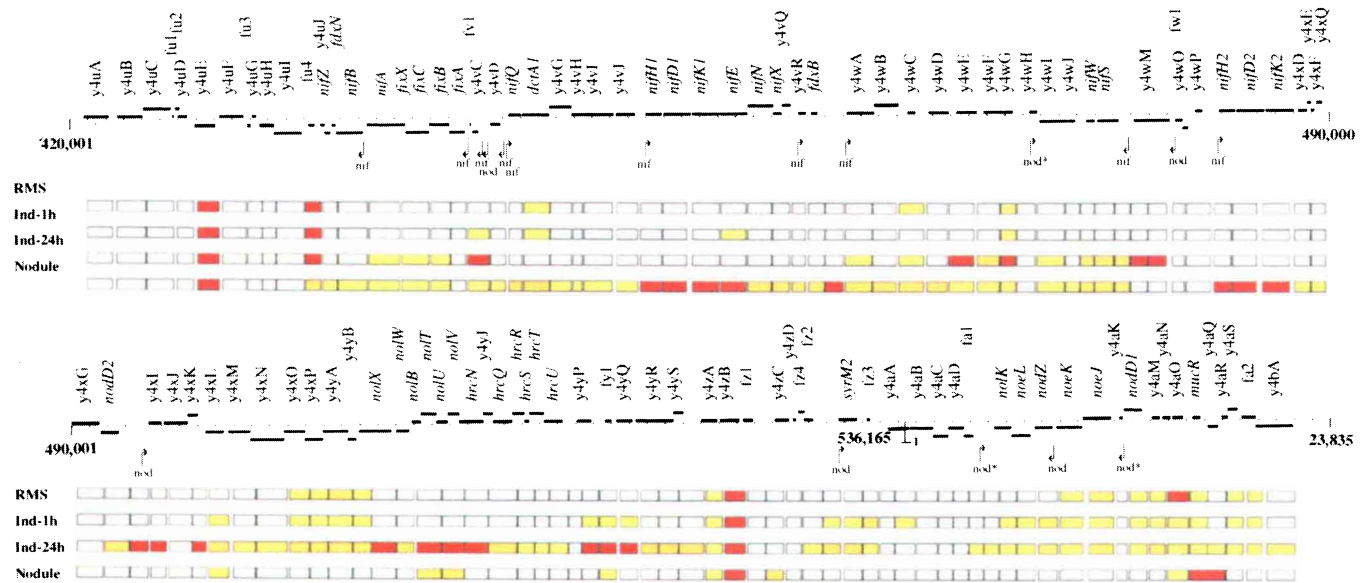


Figure 5 High-resolution transcription map of the 137-kb region encompassing the *nif* and *fix* clusters as well as the *hsnI* locus. Predicted coding regions and gene fragments are shown on each strand (black rectangles). Positions of the corresponding amplified fragments are shown directly under the ORF map. Positions and orientations of the putative *nod*-box (*nod*) and NifA- σ^{54} (*nif*) promoter sequences are marked with arrows. Probable non-functional *nod* boxes are marked with asterisks. RNA probes were prepared from: RMS, NGR234 cells

grown at 28°C in liquid *Rhizobium* minimal supplemented with succinate (RMS)²³ medium; Ind-1h, cells grown in RMS followed by a 1-h induction with 2×10^{-7} M daidzein; Ind-24h, RMS-grown rhizobia collected 24h after induction with daidzein; Nodule, bacteroids purified from Fix⁺ nodules of *V. unguiculata* inoculated with NGR234. Intensity of the hybridization signals detected on autoradiograms are colour coded as follows: yellow, weak; orange, medium; red, strong; and white, no signal.

different ways: they could 'pick up and carry' symbiotic or pathogenicity genes from one organism to another by forming composite transposons, or induce deletions, duplications, inversions and replicon fusions³¹. Unfortunately, there is no formal proof that the insertion and mosaic sequences of NGR234 have played these roles, although it seems likely, given the mosaic structure of the replicon. A striking example is the cytochrome P450 cluster (y4kS to y4kV, and y4lA to y4lD) which is 10% richer in G+C content than the rest of the plasmid, and has proteins with 83–93% similarity to those of *Bradyrhizobium*. Thus conjugal transfer and transposition have probably directed the evolution of bacteria which in one case learned genetically to colonize plants, and in the other to enter them. □

Methods

Sequencing and sequence analysis. Dye-terminator methods were used to 'shotgun' sequence a canonical array of cosmids⁷. Coding regions were detected using a mixture of intrinsic and extrinsic methods³². GeneMark predictions were based on matrices developed for *R. leguminosarum* and *R. meliloti*. BLAST and FASTA were used for similarity searches against Swiss-Prot, TrEMBL, GenBank and EMBL. Signal sequences, transmembrane segments and other characteristic domains were identified in putative proteins using the PC/Gene package. Definitions of protein families can be retrieved from the Prosite database (<http://www.expasy.ch/sprot/prosite.html>)¹². Scans for homologies were last performed in November 1996 using resources at NCBI (<http://ncbi.nlm.nih.gov>), ExPASy (<http://expasy.ch>) and EBI (www.ebi.ac.uk). Searches for consensus promoter sequences were performed using FINDPATTERNS (WASP version 8, Genetics Computer Group, Madison, Wisconsin).

Transcription analysis. We made 113 PCR products ranging from ~600 bp to ~2,000 bp between y4uA (5'-end, bp 420,774) and y4bA (3'-end, bp 21,758) using cosmid DNA as the template and primer pairs designed to amplify the discrete ORFs or intergenic regions. In some cases, M13 phage DNA (from the sequencing libraries) was used to produce PCR products. Portions of the amplified fragments were then separated on 0.8% agarose gels, and vacuum-blotted onto GeneScreen Plus Nylon membranes (NEN).

RNA extraction, labelling and hybridizations. Cell cultures at an absorbance at 600 nm of 0.4–0.5 were collected by centrifugation. Bacteroids were isolated from nodules crushed in liquid nitrogen and resuspended in sterile water. Debris was removed by filtration and bacteroids were recovered by centrifugation (4,000g, 5 min). Purification, radioactive labelling of RNA from bacteroids and collected cells, and hybridization conditions were as described¹⁸. No unlabelled competitor RNA was added to the prehybridization solution. Filters were exposed for 6–72 h, and the hybridization signals were grouped according to intensity: no signal, weak, medium and strong.

Received 14 February; accepted 14 April 1997.

1. Fellay, R., Rochepeau, P., Relić, B. & Broughton, W. J. in *Pathogenesis and Host Specificity in Plant Diseases. Histopathological, Biochemical, Genetic and Molecular Bases* (eds Singh, U. S., Singh, R. P. & Kohmoto, K.) 199–220 (Pergamon, Oxford, 1995).
2. Spaink, H. P. Regulation of plant morphogenesis by lipo-chitin oligosaccharides. *Crit. Rev. Plant Sci.* **15**, 559–582 (1996).
3. Dénarié, J., Debéllé, F. & Promé, J.-C. *Rhizobium* lipo-chitooligosaccharide nodulation factors: signalling molecules mediating recognition and morphogenesis. *Annu. Rev. Biochem.* **65**, 503–535 (1996).
4. Fischer, H.-M. Genetic regulation of nitrogen fixation in rhizobia. *Microbiol. Rev.* **58**, 352–386 (1994).
5. Lewin, A. et al. Multiple host-specificity loci of the broad host-range *Rhizobium* sp. NGR234 selected using the widely compatible legume *Vigna unguiculata*. *Plant Mol. Biol.* **8**, 447–459 (1987).
6. Broughton, W. J., Heycke, N., Meyer z.A., H. & Pankhurst, C. E. Plasmid-linked *nif* and "nod" genes in fast-growing rhizobia that nodulate *Glycine max*. *Psophocarpus tetragonolobus*, and *Vigna unguiculata*. *Proc. Natl. Acad. Sci. USA* **81**, 3093–3097 (1984).
7. Freiberg, C., Perret, X., Broughton, W. J. & Rosenthal, A. Sequencing the 500-kb GC-rich symbiotic replicon of *Rhizobium* sp. NGR234 using dye terminators and a thermostable "Sequenase": a beginning. *Genome Res.* **6**, 590–600 (1996).
8. Perret, X., Broughton, W. J. & Brenner, S. Canonical ordered cosmid library of the symbiotic plasmid of *Rhizobium* species NGR234. *Proc. Natl. Acad. Sci. USA* **88**, 1923–1927 (1991).
9. Fraser, C. M. et al. The minimal gene complement of *Mycoplasma genitalium*. *Science* **270**, 397–403 (1995).
10. Fleischmann, R. D. et al. Whole-genome random sequencing and assembly of *Haemophilus influenzae* Rd. *Science* **269**, 496–512 (1995).
11. Morrison, N. A. et al. Mobilization of a *sym* plasmid from a fast-growing cowpea *Rhizobium* strain. *J. Bacteriol.* **160**, 483–487 (1984).
12. Bairoch, A., Bucher, P. & Hofmann, K. The PROSITE database, its status in 1995. *Nucleic Acids Res.* **24**, 189–196 (1996).
13. Zhang, L., Murphy, P. J., Kerr, A. & Tate, M. E. *Agrobacterium* conjugation and gene regulation by N-acyl-L-homoserine lactones. *Nature* **362**, 446–448 (1993).
14. Piper, K. R., Beck von Bodman, S. & Farrand, S. K. Conjugation factor of *Agrobacterium tumefaciens* regulates Ti plasmid transfer by autoinduction. *Nature* **362**, 448–450 (1993).

15. Price, N. P. J. et al. Broad-host-range *Rhizobium* species strain NGR234 secretes a family of carbamoylated and fucosylated, nodulation signals that are O-acetylated or sulphated. *Mol. Microbiol.* **6**, 3575–3584 (1992).
16. Leigh, J. A. & Walker, G. C. Exopolysaccharides of *Rhizobium*: synthesis, regulation and symbiotic function. *Trends Genet.* **10**, 63–67 (1994).
17. Hanin, M. et al. Sulphation of *Rhizobium* sp. NGR234 Nod factors is dependent on *noeE*, a new host specificity gene. *Mol. Microbiol.* (in the press).
18. Fellay, R., Perret, X., Viprey, V., Broughton, W. J. & Brenner, S. Organization of host-inducible transcripts on the symbiotic plasmid of *Rhizobium* sp. NGR234. *Mol. Microbiol.* **16**, 657–667 (1995).
19. Jabbouri, S. et al. Involvement of *nodS* in N-methylation and *nodU* in 6-O-carbamoylation of *Rhizobium* sp. NGR234 Nod factors. *J. Biol. Chem.* **270**, 22968–22973 (1995).
20. van Slooten, J. C., Cervantes, E., Broughton, W. J., Wong, C. H. & Stanley, J. Sequence and analysis of the *rpoN* sigma factor gene of *Rhizobium* sp. strain NGR234, a primary coregulator of symbiosis. *J. Bacteriol.* **172**, 5563–5574 (1990).
21. Badenoch-Jones, J., Holton, T. A., Morrison, C. M., Scott, K. F. & Shine, J. Structural and functional analysis of nitrogenase genes from the broad-host range *Rhizobium* strain ANU240. *Gene* **77**, 141–153 (1989).
22. van Slooten, J. C., Bhuvanavari, T. V., Bardin, S. & Stanley, J. Two C4-dicarboxylate transport systems in *Rhizobium* sp. NGR234: rhizobial dicarboxylate transport is essential for nitrogen fixation in tropical legume symbiosis. *Mol. Plant Microbe Interact.* **5**, 179–186 (1992).
23. Broughton, W. J. et al. Identification of *Rhizobium* plasmid sequences involved in recognition of *Psophocarpus*, *Vigna*, and other legumes. *J. Cell Biol.* **102**, 1173–1183 (1986).
24. Jabbouri, S. et al. in *The Biology of Plant-Microbe Interactions* (eds Stacey, G., Mullin, B. & Gresshoff, P.) 319–324 (International Society of Molecular Plant-Microbe Interactions, St Paul, MN, 1996).
25. Krishnan, H. B., Kuo, C.-I. & Pueppke, S. G. Elaboration of flavonoid-induced proteins by the nitrogen-fixing soybean symbiont *Rhizobium fredii* is regulated by both *nodD1* and *nodD2*, and is dependent on the cultivar-specificity locus, *noXWBTUV*. *Microbiology* **141**, 2245–2251 (1995).
26. Broughton, W. J., Dilworth, M. J. & Passmore, I. K. Base ratio determination using unpurified DNA. *Anal. Biochem.* **46**, 164–172 (1972).
27. Broughton, W. J., Samrey, U. & Stanley, J. Ecological genetics of *Rhizobium meliloti*: symbiotic plasmid transfer in the *Medicago sativa* rhizosphere. *FEMS Microbiol.* **40**, 251–255 (1987).
28. Sullivan, J. T., Patrick, H. N., Lowther, W. L., Scott, D. B. & Ronson, C. W. Nodulating strains of *Rhizobium loti* arise through chromosomal symbiotic gene transfer in the environment. *Proc. Natl. Acad. Sci. USA* **92**, 8985–8989 (1995).
29. Martinez-Romero, E. & Cabellero-Mellado, J. *Rhizobium* phylogenies and bacterial genetic diversity. *Crit. Rev. Plant Sci.* **15**, 113–140 (1996).
30. Tepfer, D. in *Plant Microbe Interactions* (eds Kosuge, T. & Nester, E.) 294–342 (McGraw Hill, New York, 1989).
31. Galas, D. J. & Chandler, M. in *Mobile DNA* (eds Berg, D. E. & Howe, M. M.) 109–162 (American Society of Microbiology, Washington DC, 1989).
32. Borodovsky, M., Rudd, K. E. & Koonin, E. V. Intrinsic and extrinsic approaches for detecting genes in a bacterial genome. *Nucleic Acids Res.* **22**, 4756–4767 (1994).

Acknowledgements. We thank E. Michaelis, D. Schnabelrauch, S. Landmann, S. Förste, K. Blechschmidt and G. Nordsiek for technical assistance; B. Drescher and D. Bauer for computational assistance; M. Y. Borodovsky and W. S. Hayes for GeneMark matrices; O. White for helping to create Fig. 1; S. Farrand and P. Murphy for advice on the conjugal transfer experiments; D. Gerber and S. Relić for help with many aspects of this work; and P. Rochepeau and V. Viprey for making their unpublished data available.

Correspondence and requests for materials should be addressed to A.R. (e-mail: arosenth@imb-jena.de). The sequence of pNGR234a has been deposited in EMBL/GenBank (accession no. U00090). Putative proteins are annotated in Swiss-Prot. Further information can be retrieved from the World-Wide Web (<http://genome.imb-jena.de/archives.html>).

Task difficulty and the specificity of perceptual learning

Merav Ahissar*† & Shaul Hochstein‡

* Center for Higher Brain Functions, Department of Neurobiology, Weizmann Institute of Science, Rehovot 76100, Israel

‡ Center for Neural Computation, Department of Neurobiology, Institute of Life Sciences, Hebrew University of Jerusalem, Jerusalem 91904, Israel

Practising simple visual tasks leads to a dramatic improvement in performing them. This learning is specific to the stimuli used for training. We show here that the degree of specificity depends on the difficulty of the training conditions. We find that the pattern of specificities maps onto the pattern of receptive field selectivities along the visual pathway. With easy conditions, learning generalizes across orientation and retinal position, matching the spatial generalization of higher visual areas. As task difficulty increases, learning becomes more specific with respect to both orientation and position, matching the fine spatial retinotopy exhibited by lower areas. Consequently, we enjoy the benefits of

† Present address: Keck Center for Integrative Neuroscience, UCSF, San Francisco, California 94143-0732, USA.